Cancer Science

WILEY | JCA JAPANESE CANCER ASSOCIATION

ORIGINAL ARTICLE OPEN ACCESS

Microtubule Inhibitors Induce Cross-Resistance to Osimertinib Through CaMKII Activation in EGFR-Mutated NSCLC

Kento Kono | Ryosuke Tanino | Yukari Tsubata | Eshat Fahmida Haque | Takeshi Isobe | Tamio Okimoto

Division of Medical Oncology and Respiratory Medicine, Department of Internal Medicine, Shimane University Faculty of Medicine, Izumo, Japan

Correspondence: Tamio Okimoto (okimoto@med.shimane-u.ac.jp)

Received: 23 June 2025 | **Revised:** 6 November 2025 | **Accepted:** 14 November 2025

Keywords: calcium/calmodulin-dependent protein kinase II | non-small cell lung cancer | osimertinib | paclitaxel | vinorelbine

ABSTRACT

The current standard postoperative adjuvant therapy for patients with epidermal growth factor receptor (EGFR)-mutated non-small cell lung cancer (NSCLC) includes chemotherapy, including microtubule inhibitors prior to the administration of osimertinib, an EGFR-tyrosine kinase inhibitor (TKI). However, multidrug resistance following treatment with microtubule inhibitors has been reported, and the optimal sequence of drug administration for EGFR-mutated NSCLC remains undefined. In this study, we investigated whether prior treatment with microtubule inhibitors induces acquired cross-resistance to osimertinib in EGFR-mutated NSCLC cells in vitro. To model acquired resistance, PC-9 cells were exposed to vinorelbine or paclitaxel for 18 weeks—approximating the clinical duration of four adjuvant chemotherapy cycles—and subsequent drug sensitivity and signaling pathway alterations were assessed using cell viability assays, RNA sequencing, and immunoblotting. We found that two human NSCLC cell lines derived from PC-9 exhibited reduced sensitivity to osimertinib after 18 weeks of in vitro treatment with tubulin inhibitors: vinorelbine (PC-9/VNR) and paclitaxel (PC-9/PTX). Furthermore, PC-9/VNR and PC-9/PTX cells showed activation of FZD7 and calcium/calmodulin-dependent protein kinase II (CaMKII), along with increased sensitivity to the CaMKII inhibitor KN-93, which exerted additive or synergistic effects. These findings suggest that CaMKII plays a critical role in EGFR-TKI resistance. This study underscores the importance of optimizing the timing of EGFR-TKI administration in the therapeutic sequence for EGFR-mutated NSCLC.

1 | Introduction

Non-small cell lung cancer (NSCLC) accounts for approximately 85% of all lung cancer cases and is the leading cause of cancer-related death worldwide [1]. Postoperative adjuvant chemotherapy, traditionally involving cytotoxic agents such as microtubule inhibitors, remains a standard treatment for patients with completely resected stage I–III NSCLC [2, 3]. With routine implementation of molecular testing for oncogene driver variants of NSCLC tumors, osimertinib—a third-generation epidermal growth factor receptor (EGFR)-tyrosine kinase inhibitor (TKI) (EGFR-TKI)—is now widely administered to patients with EGFR-mutated NSCLC [4]. Adjuvant osimertinib has been shown to improve the 5-year overall survival rate by 10% in patients with stage IB to IIIA EGFR-mutated NSCLC following complete resection and is recommended based on results from the phase III ADAURA trial [5]. In ADAURA, patients were randomized 1:1 to receive osimertinib or placebo for

Abbreviations: DEGs, differentially expressed genes; EGFR, epidermal growth factor receptor; FDR, false discovery rate; GSEA, Gene Set Enrichment Analysis; NSCLC, non-small cell lung cancer; PTX, paclitaxel; RNA-seq, RNA sequencing; TBS-T, 0.05% Tween-20 in TBS; TKI, tyrosine kinase inhibitor; VNR, vinorelbine; ZIP, zero interaction potency.

3 years, and adjuvant chemotherapy prior to randomization was optional, determined by physician and patient choice. A subgroup analysis demonstrated comparable outcomes regardless of whether patients received prior adjuvant chemotherapy [6]. However, whether adjuvant chemotherapy followed by osimertinib administration represents the optimal therapeutic strategy remains controversial [6–8]. The ideal sequence of therapies, including the necessity of adjuvant chemotherapy, remains to be defined. Therefore, further investigation into the efficacy of adjuvant treatment with other EGFR-TKIs and chemotherapeutic agents in NSCLC is essential to establish the most effective therapeutic approach.

The development of multidrug resistance following the administration of microtubule inhibitors, such as vinorelbine (VNR) and paclitaxel (PTX), has been widely reported. Treatment with these agents can upregulate the expression of a drug-efflux transporter ATP-binding cassette sub-family B member 1 [9, 10] and promote epithelial–mesenchymal transition—a process characterized by the acquisition of mesenchymal traits and histologically associated with drug resistance in epithelial-derived NSCLC cells [11]. Furthermore, acquired EGFR-TKI resistance commonly emerges following EGFR-TKI treatment. While the EGFR T790M mutation is a common mechanism, various EGFR-independent pathways of acquired EGFR-TKI resistance have been reported [12]. However, owing to limited knowledge regarding how resistance to tubulin inhibitors affects the efficacy of EGFR-TKIs in EGFR-mutated NSCLC, further investigation is warranted.

We hypothesized that adjuvant tubulin inhibitor therapy may diminish the efficacy of EGFR-TKIs owing to cross-resistance acquired during prior treatment. To test this hypothesis, we investigated whether treatment with microtubule inhibitors induces acquired cross-resistance to osimertinib in EGFR-mutated NSCLC cells in vitro. This study provides experimental evidence regarding how prior exposure to microtubule inhibition may influence subsequent therapeutic strategies for patients with EGFR-mutated NSCLC.

2 | Materials and Methods

2.1 | Cell Culture

EGFR-mutated (delE746_A750 and L858R/T790M) cell lines, PC-9 and H1975, derived from human lung adenocarcinoma, were maintained in RPMI 1640 medium supplemented with 10% (v/v) FBS and 50 μg/mL gentamicin in a humidified incubator at 37°C with 5% CO_2. Genetic authentication of the PC-9 cell line was performed using the PowerPlex 16 STR system (Promega, Madison, WI, USA). VNR, PTX, osimertinib, and KN-93 were purchased from Selleck Chemicals (Houston, TX, USA) and dissolved in DMSO.

2.2 | Establishment of Drug-Treated Cell Lines via 18-Week Microtubule Inhibitor Exposure

An 18-week continuous treatment regimen was selected to model the clinical exposure associated with four cycles of adjuvant chemotherapy. Cells were seeded at a density of 4000 cells/cm^2 following each passage and treated with VNR or PTX added to the culture medium. The stepwise increase in drug concentration was used to mimic gradual resistance development while maintaining cell viability. The initial concentrations of VNR and PTX were set at 3.0 and 6.0 nM for PC-9 and H1975 cells, respectively, which were slightly lower than the half-maximal inhibitory concentrations determined in preliminary assessments (PC-9: 5.3 nM for VNR and 5.0 nM for PTX; H1975: 12 nM for VNR and 13 nM for PTX). The concentration was incrementally increased when proliferating cells reached confluence within 3 days of each seeding. VNR or PTX treatment was continued for 18 weeks without interruption. Following the treatment period, the cell lines were maintained without VNR or PTX and designated as PC-9/VNR or PC-9/PTX for PC-9-derived cells and H1975/VNR or H1975/PTX for H1975-derived cells.

2.3 | Cell Viability Assay

Cells were seeded at a density of 3000 cells/cm^2 in 96-well tissue culture plates with the indicated drug concentrations. Following the specified duration of treatment, 10 μL of Cell Counting Kit-8 reagent (Dojindo, Mashiki, Japan) was added to each well and incubated at 37°C with 5% CO_2 for 2 h. Absorbance was measured at 450 and 640 nm using a microplate reader, and the difference (450–630 nm) was used as the measurement value. Cell viability (%) was calculated using the following formula: 100 × (measurement value of the treated sample/measurement value of the vehicle control).

2.4 | Immunoblotting

Cells were lysed using Mammalian Protein Extraction Reagent (Thermo Fisher Scientific, Waltham, MA, USA) supplemented with 1% (v/v) Phosphatase Inhibitor Cocktail (Nacalai Tesque, Kyoto, Japan) and 1% (v/v) Protease Inhibitor Cocktail (Thermo Fisher Scientific), after a 24-h treatment with the indicated drugs. Protein samples were mixed with LDS Sample Buffer and Sample Reducing Agent (both from Thermo Fisher Scientific), then heated at 95°C for 5 min. Samples were loaded onto Tris–glycine gels. Following electrophoresis and transfer to nitrocellulose membranes, the membranes were blocked with 5% non-fat milk at 20°C–25°C for 1 h, followed by 14–18 h incubation at 4°C with primary antibodies in a diluent of 5% non-fat milk or 1% bovine serum albumin in 0.05% Tween-20 containing Tris-buffered saline (TBS-T). After three washes with TBS-T, the membranes were incubated with horseradish peroxidase-conjugated secondary antibodies (anti-rabbit IgG [Cytiva, Tokyo, Japan; NA934, 1:30,000] or anti-mouse IgG [Cytiva; NA931, 1:10,000]) in TBS-T at 20°C–25°C for 1 h and washed three times with TBS-T. Target proteins were visualized using ECL Select Detection Reagent (Cytiva) and imaged with an Amersham ImageQuant 800 system (Cytiva). The primary antibodies used were as follows: anti-EGFR (Cell Signaling Technology [CST], Danvers, MA, USA; #4267, 1:500), anti-phospho-$EGFR^{Tyr1068}$ (CST; #3777, 1:1000), anti-Akt1/2/3 (Santa Cruz Biotechnology [SCBT]; sc-8312, 1:500), anti-phospho-Akt^{Ser473} (CST; #4060, 1:2000), anti-Erk1/2

(CST; #4695, 1:2000), anti-phospho-Erk1/2$^{Thr202/Tyr204}$ (CST; #4370, 1:2000), anti-phospho-CaMKII^{Thr286} (CST; #12716, 1:1000), anti-PARP (CST; #9532, 1:1000), anti-Wnt5a (SCBT; sc-365,370, 1:500), anti-Frizzled-7 (SCBT; sc-293,261, 1:500), and anti-GAPDH (CST; #8884, 1:3000). Band intensity was quantified using ImageJ software (version 1.54p; National Institutes of Health, MD, USA).

2.5 | RNA Sequencing (RNA-seq) Analysis

Total RNA was extracted from cultured cells using the RNeasy Mini Kit (Qiagen, Hilden, Germany) according to the manufacturer's instructions. RNA-seq samples were prepared using the SMART-Seq v4 Ultra Low Input RNA Kit (Takara Bio, Kusatsu, Japan), which transcribes mRNAs into cDNAs. Library preparation was conducted using the Nextera XT DNA Library Preparation Kit (Illumina, San Diego, CA, USA). Paired-end 150-base reads were sequenced using the NovaSeq 6000 sequencing platform (Illumina).

2.6 | Gene Set Enrichment Analysis (GSEA)

GSEA was selected for its robust ability to detect coordinated changes in gene sets, even when individual genes do not reach statistical significance. GSEA software (version 4.3.3) was downloaded from the Broad Institute's GSEA portal (https://www.gsea-msigdb.org/gsea/index.jsp). RNA-seq gene expression data from each cell line were analyzed to identify pathways associated with the 18-week VNR or PTX treatment. Gene signatures were obtained from the Molecular Signatures Database (https://www.gsea-msigdb.org/gsea/msigdb/index.jsp). Gene sets with a p-value <0.05 and a false discovery rate (FDR) q-value <0.25 were considered statistically significant.

2.7 | Cell Cycle Analysis

Following treatment with DMSO or KN-93 for 48 h, cells were incubated with 1 μM BrdU of the BrdU Flow kit (BD Biosciences, Franklin Lakes, NJ, USA) for 90 min, washed with PBS, and harvested. Cell fixation, permeabilization, DNase treatment, fluorescein-conjugated anti-BrdU antibody labeling, and 7-aminoactinomycin D DNA staining were performed using the BrdU Flow Kit (BD Biosciences). Flow cytometry was conducted using a CytoFLEX cytometer (Beckman Coulter, Brea, CA, USA). Cell cycle distribution was quantified using the CytExpert software (Beckman Coulter).

2.8 | Colony Formation Assay

Cells were seeded in 6-well plates at a density of 400 cells per well. After 1 week of preculture, the cells were treated with KN-93 or DMSO alone at 37°C with 5% CO_2 for 72 h. Colonies were fixed with 4% formaldehyde at 20°C–25°C for 10 min, stained with 0.5% crystal violet in 20% methanol at 20°C–25°C for 10 min, washed 10 times with distilled water, and incubated at 20°C–25°C until dry. Following imaging of the stained colonies, 400 μL of 30% acetic acid was added to each well, and the plates were shaken at 300 rpm for 5 min to dissolve the crystal violet. Absorbance of the dissolved crystal violet was measured at 595 nm.

2.9 | Cell Invasion Assay

The membranes of TC Inserts with 8-μm pores (Sarstedt; Nümbrecht, Germany) were coated with 10% Matrigel Matrix (Corning Inc, Corning, NY, USA) in PBS and incubated at 20°C–25°C for 1 h. Cells were seeded at a density of 4.5×10^4 per insert in FBS-free culture medium. Each insert was placed into a well of a 24-well culture plate with FBS-supplemented culture media. Following incubation at 37°C for 48 h, non-invasive cells remaining on the upper surface of the membrane were removed using a cotton swab. Invaded cells on the underside of the membrane were fixed with 4% paraformaldehyde at 20°C–25°C for 10 min and stained with Diff-Quik (Sysmex, Kobe, Japan; 16920). The stained cells were counted in 10 non-overlapping fields per group using a 20× objective under a light microscope.

2.10 | siRNA Transfection

Pre-designed Silencer Select siRNAs targeting CaMKII (CaMKII#1, s2358; CaMKII#2, s2359; Thermo Fisher Scientific, Waltham, MA, USA) were used to achieve CaMKII knockdown. Silencer Select Negative Control siRNA (Thermo Fisher Scientific) served as a negative control. Cells were seeded in 60-mm dishes, and siRNA transfection was performed using ScreenFect A plus reagent (Fujifilm Wako, Osaka, Japan) according to the manufacturer's instructions. The siRNA–lipid complexes were prepared in culture medium at a final siRNA concentration of 10 nM and added dropwise to the cells. The cells were incubated for 72 h and subsequently harvested for immunoblotting and CCK-8 assays.

2.11 | Analysis of Effects of Drug Combination

Synergistic inhibitory effects of osimertinib and KN-93 were evaluated using SynergyFinder (version 3.0) software with the zero interaction potency (ZIP) model, which calculates a ZIP synergy score [13]. The ZIP model was selected for its ability to capture both the potency and interaction patterns of drug combinations, providing a more comprehensive synergy assessment. A ZIP synergy score of less than −10 indicates an antagonism between the drugs, a score between −10 and 10 suggests an additive effect, and a score greater than 10 indicates a synergy.

2.12 | Statistical Analysis

All statistical analyses were performed using Prism (GraphPad Software, Boston, MA, USA; version 9.3.1). The Kruskal–Wallis test was applied to compare three independent groups. A two-sided p-value <0.05 was considered statistically significant.

3 | Results

3.1 | Long-Term Exposure to Tubulin Inhibitors Induces Acquired Resistance to Osimertinib

PC-9 cells were cultured with VNR or PTX for 18 weeks. By week 12—corresponding to approximately three cycles of adjuvant chemotherapy—the concentrations of VNR and PTX were 15.0 and 7.0 nM, respectively. By week 18—equivalent to approximately four cycles of chemotherapy—their concentrations were 20.0 and 8.0 nM, respectively (Figure 1A). A cell viability assay was used to assess acquired drug resistance. PC-9/VNR and PC-9/PTX cells demonstrated time-dependent increases in resistance to VNR and PTX, respectively, compared to parental PC-9 cells (Figure 1B). Furthermore, both cell lines exhibited higher resistance to each microtubule inhibitor after 18 weeks than after 12 weeks of treatment (Figure 1B). Importantly, both lines developed concomitant resistance to osimertinib, compared to the parental PC-9 cells, following 18 weeks of treatment with their respective tubulin inhibitors (Figure 2A). To confirm the inhibitory effect of osimertinib on EGFR signaling, we evaluated the phosphorylation of EGFR and its downstream proteins, ERK and AKT. Osimertinib inhibited EGFR phosphorylation in all cell lines (Figure 2B). However, AKT and ERK phosphorylation was elevated in PC-9/VNR and PC-9/PTX cells, and ERK phosphorylation was not suppressed by osimertinib to the same extent as in PC-9 cells (Figure 2B). These results indicate that prolonged exposure to tubulin inhibitors not only induces resistance to the respective agents but also leads to cross-resistance to osimertinib, potentially through sustained ERK pathway activation.

3.2 | The Non-Canonical Wnt Signaling Pathway Is Upregulated in Tubulin Inhibitor–Resistant Cell Lines

To investigate signaling pathways contributing to the acquired resistance to osimertinib in PC-9/VNR and PC-9/PTX cells, we performed gene expression analysis using RNA-seq. Plots of significant differentially expressed genes (DEGs) relative to those in parental PC-9 cells are shown in Figure 3A. Among the upregulated DEGs, *WNT5a*, a known oncogene [14], was notably elevated in both PC-9/VNR and PC-9/PTX cells (Tables S1 and S2). Based on this, we performed GSEA to assess Wnt signaling-related gene signatures. The PID_WNT_NONCANONICAL_PATHWAY gene set was significantly enriched in PC-9/VNR cells, while both PID_WNT_SIGNALING_PATHWAY and PID_WNT_NONCANONICAL_PATHWAY were enriched in PC-9/PTX cells. In contrast, the PID_WNT_CANONICAL_PATHWAY was not significantly enriched in either cell line (Figure 3B). Furthermore, the expression of key proteins associated with the non-canonical Wnt/Ca^{2+} pathway—Wnt5a and FZD7—was elevated in PC-9/VNR and PC-9/PTX cells (Figure 3C).

These findings suggest that activation of the non-canonical Wnt/Ca^{2+} signaling pathway may contribute to the acquired resistance phenotype observed in tubulin inhibitor–resistant PC-9 cells. In addition, H1975 cells were cultured with VNR or PTX for 18 weeks in the same manner as PC-9 cells, reaching final concentrations of 10 nM for both VNR and PTX. However, H1975-derived cells (H1975/VNR and H1975/PTX) did not

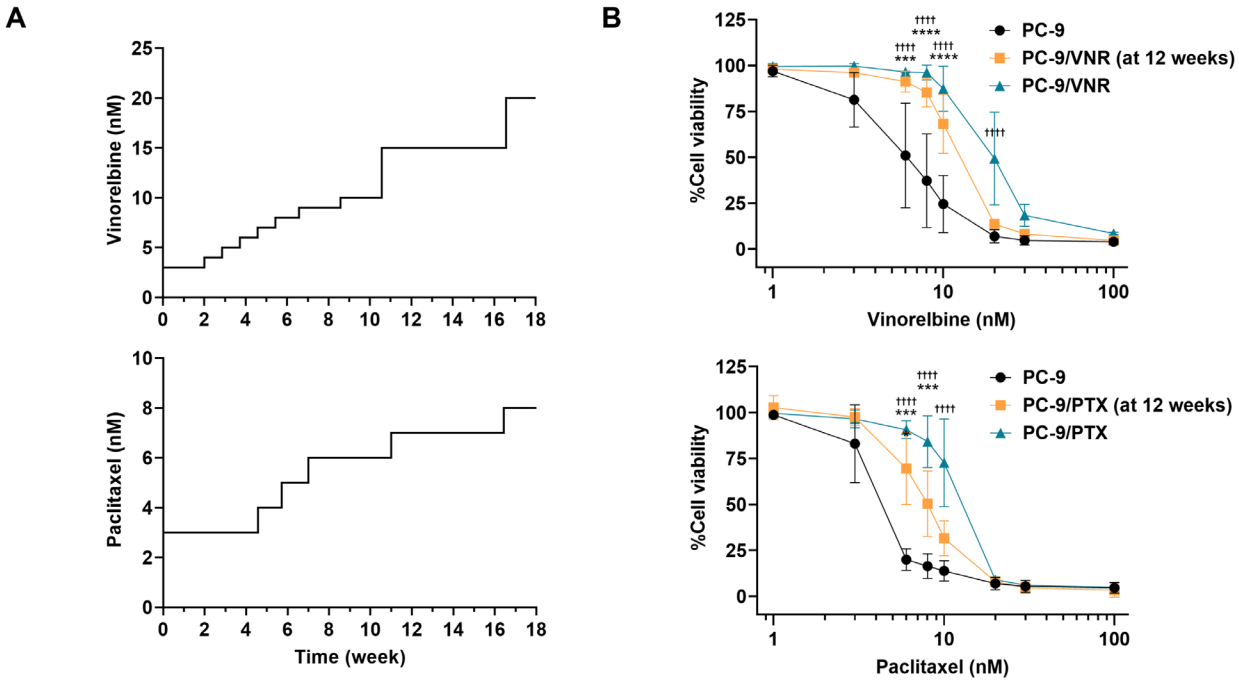

FIGURE 1 | Long-term in vitro exposure to tubulin inhibitors induces acquired resistance to osimertinib in the human non-small cell lung cancer cell line, PC-9. (A) Stepwise increases in the concentrations of vinorelbine (VNR) or paclitaxel (PTX) result in resistant PC-9 lines designated as PC-9/VNR and PC-9/PTX, respectively. (B) Cell viability after 72 h of VNR or PTX treatment was higher in PC-9/VNR and PC-9/PTX cells than that in parental PC-9 cells. Data are presented as mean ± SD (experimental replicates, $n = 3$). Statistical significance: PC-9 vs. PC-9/VNR or PC-9/PTX at 12 weeks, ***$p < 0.001$; ****$p < 0.0001$. PC-9 vs. PC-9/VNR or PC-9/PTX at 18 weeks, $^{\dagger\dagger\dagger\dagger}p < 0.0001$.

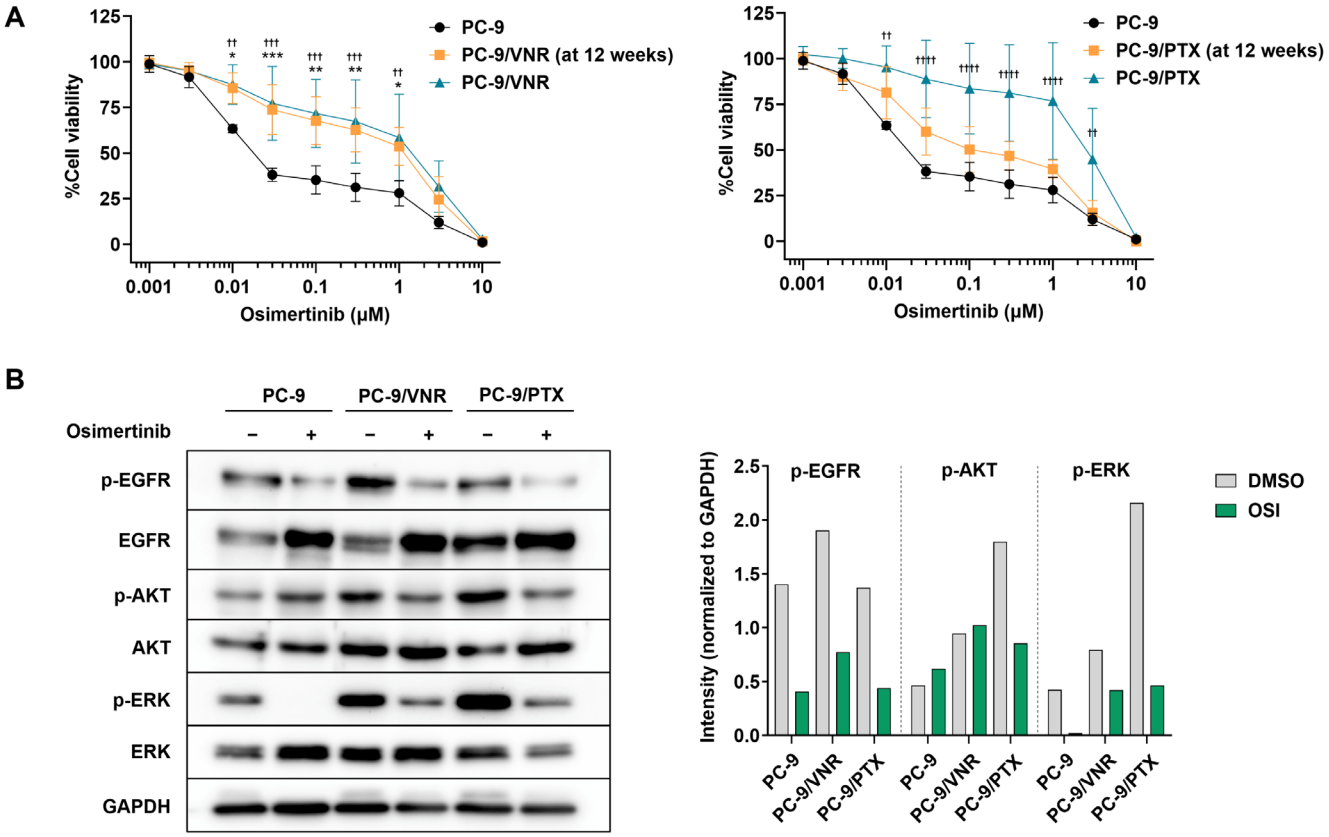

FIGURE 2 | VNR-resistant PC-9/VNR and PTX-resistant PC-9/PTX cells acquire cross-resistance to osimertinib. (A) Cell viability following 72 h of osimertinib treatment was also elevated in PC-9/VNR and PC-9/PTX cells compared to that of parental PC-9 cells. (B) Osimertinib (OSI; 10 nM, 24 h) inhibited epidermal growth factor receptor (EGFR) phosphorylation in PC-9/VNR and PC-9/PTX cells, similar to that observed in the parental PC-9 cells. Immunoblots show levels of the total and phosphorylated forms of intracellular EGFR signaling proteins. GAPDH was used as a loading control. Data are presented as mean ± SD ($n = 3$). Statistical significance: PC-9 vs. PC-9/VNR or PC-9/PTX at 12 weeks, $^{*}p < 0.05$; $^{**}p < 0.01$; $^{***}p < 0.001$. PC-9 vs. PC-9/VNR or PC-9/PTX at 18 weeks, $^{\dagger\dagger}p < 0.01$; $^{\dagger\dagger\dagger}p < 0.001$; $^{\dagger\dagger\dagger\dagger}p < 0.0001$.

exhibit any significant alterations in the non-canonical Wnt/Ca^{2+} signaling pathway (Figure S1).

3.3 | CaMKII Inhibition Suppresses Proliferation and Invasion in Microtubule Inhibitor–Treated Cells

CaMKII is the key regulatory mediator in the non-canonical Wnt/Ca^{2+} pathway [15]. To evaluate the functional relevance of this pathway in PC-9/VNR and PC-9/PTX cells, we used KN-93, a selective, cell-permeable, and competitive CaMKII inhibitor [16, 17]. Phosphorylation of CaMKII was increased in PC-9/VNR and PC-9/PTX cells but inhibited by KN-93 treatment to levels similar to those in PC-9 cells (Figure 4A). Phosphorylation of EGFR and ERK was downregulated by KN-93 treatment in PC-9, PC-9/VNR, and PC-9/PTX cells (Figure 4A). Although cleaved PARP, a marker of apoptosis, was not detected following KN-93 treatment (Figure 4A), KN-93 increased the proportion of cells in G_0/G_1 phase and decreased the proportion in S-phase (Figure 4B). However, KN-93 inhibited cell viability more strongly in PC-9/VNR and PC-9/PTX cells than in PC-9 cells (Figure 4C). In addition, CaMKII inhibition significantly reduced colony formation in PC-9/VNR and PC-9/PTX cells, but not in PC-9 cells (Figure 4D). Furthermore, KN-93 treatment decreased the number of cells invading the Matrigel-coated membrane (Figure 4E). To confirm that the inhibitory effect of KN-93 was specifically mediated through CaMKII, we performed siRNA-mediated CaMKII knockdown. Silencing CaMKII decreased its phosphorylation (Figure 4F) and reduced cell viability in PC-9/VNR and PC-9/PTX cells but not in the parental PC-9 cells (Figure 4G). Together, these results indicate that CaMKII plays a critical role in sustaining the proliferation and invasive potential of tubulin inhibitor–resistant cells and that its inhibition selectively impairs these phenotypes in drug-resistant PC-9/VNR and PC-9/PTX cells.

3.4 | Combination Therapy With Osimertinib and KN-93 Exerts a Synergistic Effect in Tubulin Inhibitor–Resistant Cell Lines

Next, we evaluated the potential synergy between KN-93 and osimertinib. The combination treatment reduced cell viability more in PC-9/VNR and PC-9/PTX cells than that in the parental PC-9 cells (Figure 5A). In addition, the combination treatment decreased phosphorylation levels of EGFR, AKT, and ERK in all three cell lines (Figure 5B). To determine whether the combination effect was synergistic or merely additive, we calculated the ZIP synergy score. The interaction was additive in PC-9 (ZIP synergy score: 5.761) and PC-9/VNR (ZIP synergy score: 5.284) cells but synergistic in PC-9/PTX cells (ZIP synergy score:

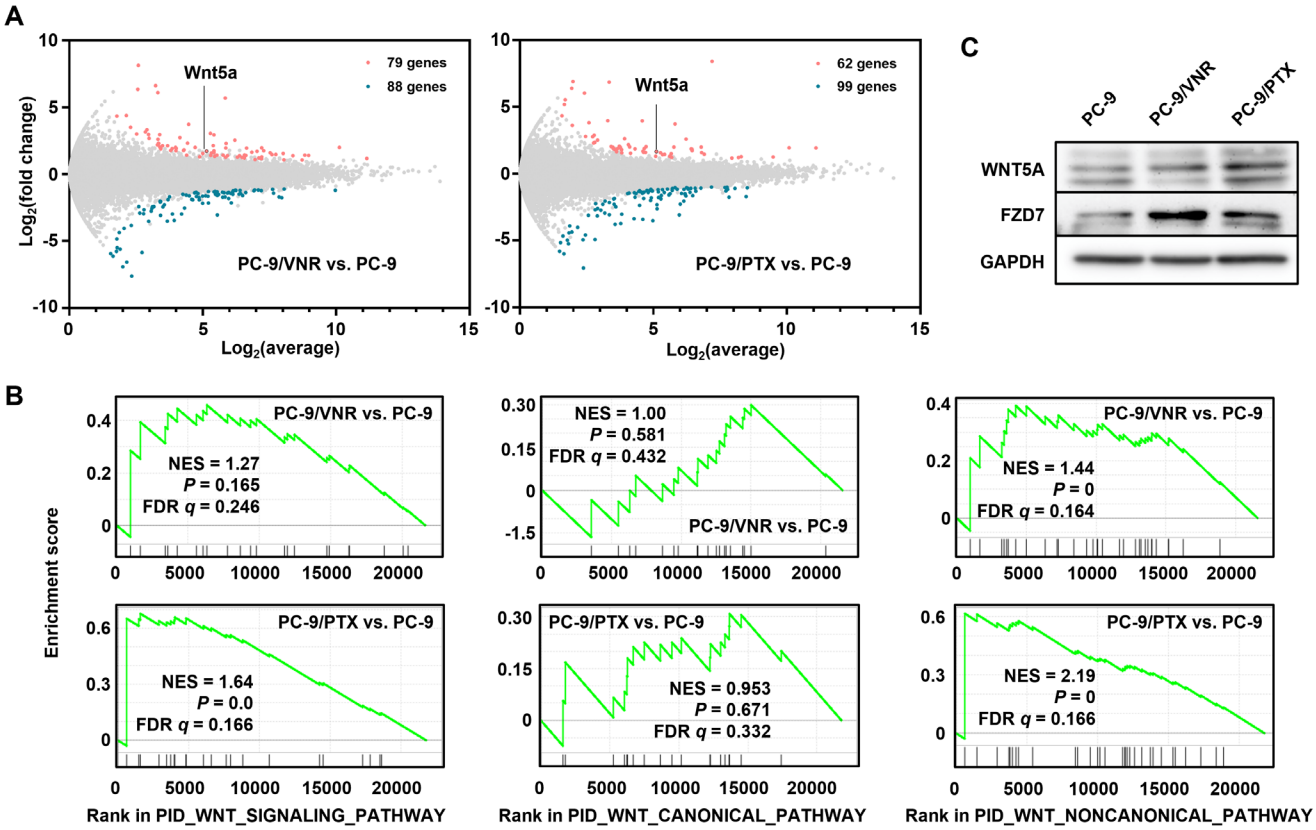

FIGURE 3 | Tubulin inhibitor–resistant cell lines (PC-9/VNR and PC-9/PTX) exhibit upregulation of non-canonical Wnt signaling-related mRNAs and proteins. (A) MA plots showing differentially expressed genes (DEGs) between PC-9 and PC-9/VNR or PC-9/PTX cells. Genes with $|\log_2(\text{fold change})| > 1$ and adjusted $p < 0.05$ were considered DEGs. Red, upregulated; blue, downregulated. (B) Gene Set Enrichment Analysis (GSEA) of RNA sequencing (RNA-seq) data comparing PC-9 with PC-9/VNR and PC-9/PTX cells. Wnt signaling-related pathways were analyzed using the Pathway Interaction Database (PID), including PID_WNT_SIGNALING_PATHWAY, PID_WNT_CANONICAL_PATHWAY, and PID_WNT_NONCANONICAL_PATHWAY. (C) Immunoblot showing expression levels of Wnt signaling proteins, Wnt5a and FZD7. FZD7 expression was higher in PC-9/VNR and PC-9/PTX cells than in PC-9 cells.

10.942) (Figure 5C). These findings suggest that combination therapy with KN-93 and osimertinib has enhanced efficacy in tubulin inhibitor–resistant cells, with a notably synergistic effect observed in paclitaxel-resistant PC-9/PTX cells.

4 | Discussion

We demonstrated for the first time that VNR- and PTX-treated NSCLC cells acquire reduced sensitivity to osimertinib—the primary therapeutic agent for EGFR-mutated NSCLC—through activation of the FZD7/CaMKII signaling axis. These findings suggest that prior adjuvant treatment with a tubulin inhibitor may compromise the subsequent efficacy of EGFR-TKIs in recurrent NSCLC. Given that treatment sequence can influence overall therapeutic outcomes in cancer, and different drug interactions could lead to varied responses and time to recurrence [18, 19], understanding drug interactions is critical. As an added challenge, acquired drug resistance frequently develops following initial clinical benefit, and the mechanisms are known to vary depending on the drug [20]. To investigate this, we developed in vitro post-adjuvant models of VNR- and PTX-treated NSCLC cells (PC-9/VNR and PC-9/PTX) and evaluated their response to osimertinib. The treatment duration of the cross-resistant cells was 18 weeks, reflecting the cumulative exposure typically seen in three or four cycles of 4-week adjuvant chemotherapy involving microtubule inhibitors [21, 22]. Following this prolonged exposure, both PC-9/VNR and PC-9/PTX cells exhibited stable cross-resistance to osimertinib. We found FZD7 overexpression and elevated CaMKII and ERK phosphorylation in PC-9/VNR and PC-9/PTX cells, despite no detectable changes in EGFR pathway activity. Moreover, treatment with the CaMKII inhibitor KN-93 suppressed cell cycle progression and invasion in both PC-9/VNR and PC-9/PTX cells, indicating that the CaMKII pathway may serve as a viable therapeutic target to overcome resistance to osimertinib.

Wnt/Ca^{2+} signaling is a β-catenin-independent, non-canonical Wnt pathway initiated by Wnt and Frizzled proteins, such as WNT5a and FZD7, which induce intracellular Ca^{2+} influx through Orai Ca^{2+} channels [15, 23]. In contrast, the canonical Wnt signaling pathway has been linked to EGFR-mutated NSCLC [24, 25]. Our RNA-seq analysis revealed upregulation of the non-canonical Wnt signaling pathway in PC-9/VNR and PC-9/PTX cells compared with that in PC-9 cells. Notably, Wnt/Ca^{2+} signaling can enhance Cdc42 activation, which is implicated in acquired resistance to several drugs, including PTX [26]. Sennoune et al. similarly reported that prostate cancer cells

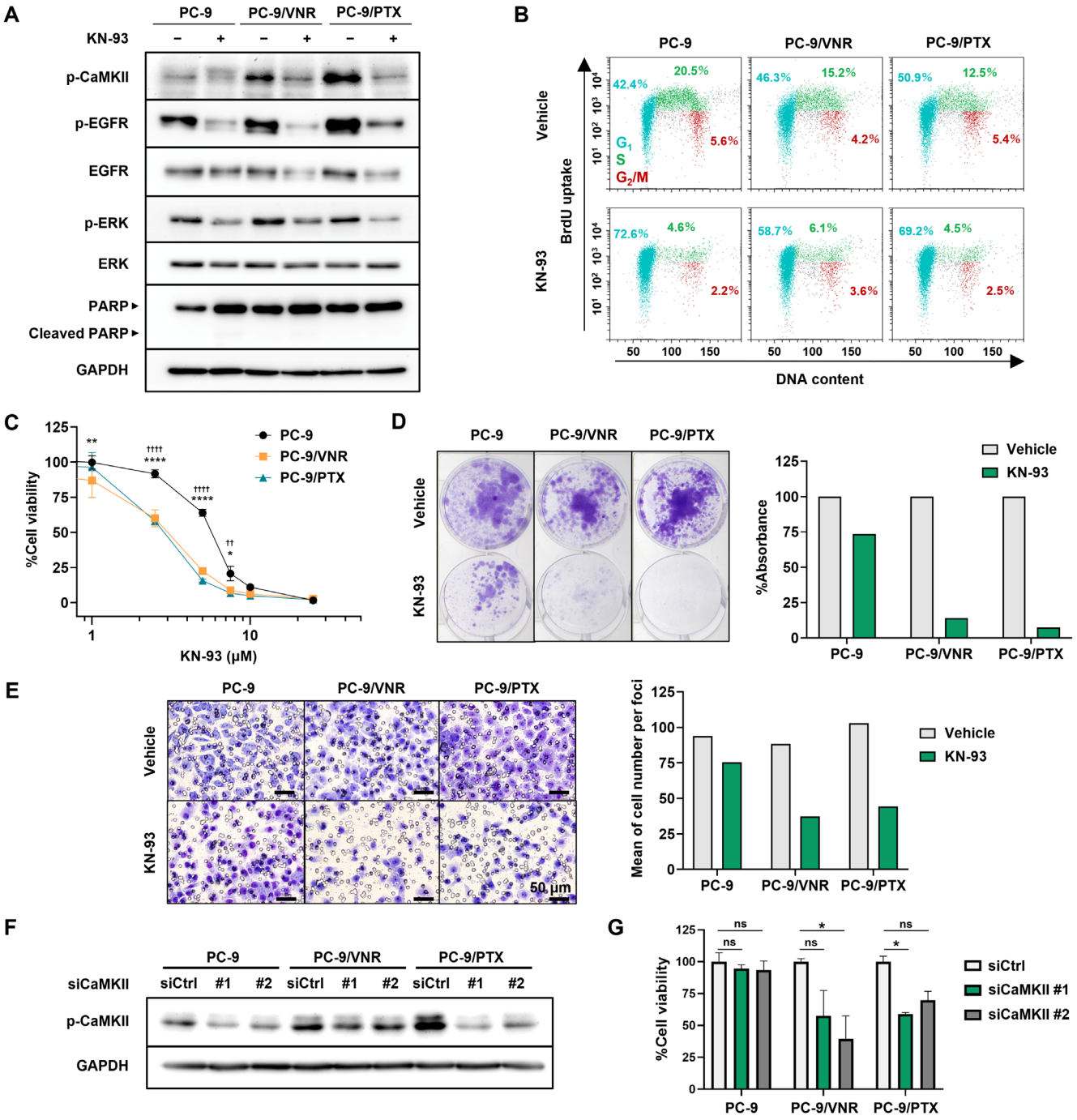

FIGURE 4 | CaMKII inhibition effectively suppresses proliferation and invasion in tubulin inhibitor-resistant PC-9/VNR and PC-9/PTX cells. (A) The CAMKII inhibitor, KN-93 (7.5 μM, 24 h), inhibited phosphorylation of CaMKII, EGFR, and ERK. (B) KN-93 (7.5 μM, 48 h) altered cell cycle distribution in PC-9, PC-9/VNR, and PC-9/PTX cells. (C) KN-93 (2.5–7.5 μM, 72 h) reduced cell viability more in PC-9/VNR and PC-9/PTX cells than in parental PC-9 cells. Data are expressed as mean ± SD ($n = 3$). Statistical significance: PC-9 vs. PC-9/VNR, $^{*}p < 0.05$; $^{**}p < 0.01$; $^{****}p < 0.0001$. PC-9 vs. PC-9/PTX, $^{\dagger\dagger}p < 0.01$; $^{\dagger\dagger\dagger\dagger}p < 0.0001$. (D) KN-93 (7.5 μM, 24 h) markedly inhibited colony formation in PC-9/VNR and PC-9/PTX cells. Representative colony images and absorbance values of crystal violet staining are shown. (E) KN-93 (7.5 μM, 48 h) inhibited cell invasion in PC-9/VNR and PC-9/PTX cells. Representative microscopy images and the mean number of invading cells per 10 non-overlapping fields are shown. (F) Phosphorylation levels of CaMKII decreased in PC-9, PC-9/VNR, and PC-9/PTX cells following transfection with CaMKII-targeting siRNA compared to those with negative control siRNA (siCtrl) transfection. (G) Cell viability decreased in PC-9/VNR and PC-9/PTX cells after CaMKII knockdown. Data are expressed as mean ± SD ($n = 3$). Statistical significance: ns, non-significant; $^{*}p < 0.05$.

treated with cabazitaxel, a taxane agent, exhibited activation of the non-canonical Wnt signaling pathway [27]. Although a direct link between Wnt/Ca^{2+} signaling and EGFR-TKI resistance remains to be clarified, NSCLC tumors with high WNT5a expression have been reported to respond poorly to EGFR-TKIs in clinical settings [28]. Collectively, these studies suggest that exposure to microtubule inhibitors may upregulate Wnt/Ca^{2+} signaling, consistent with our in vitro models. Furthermore,

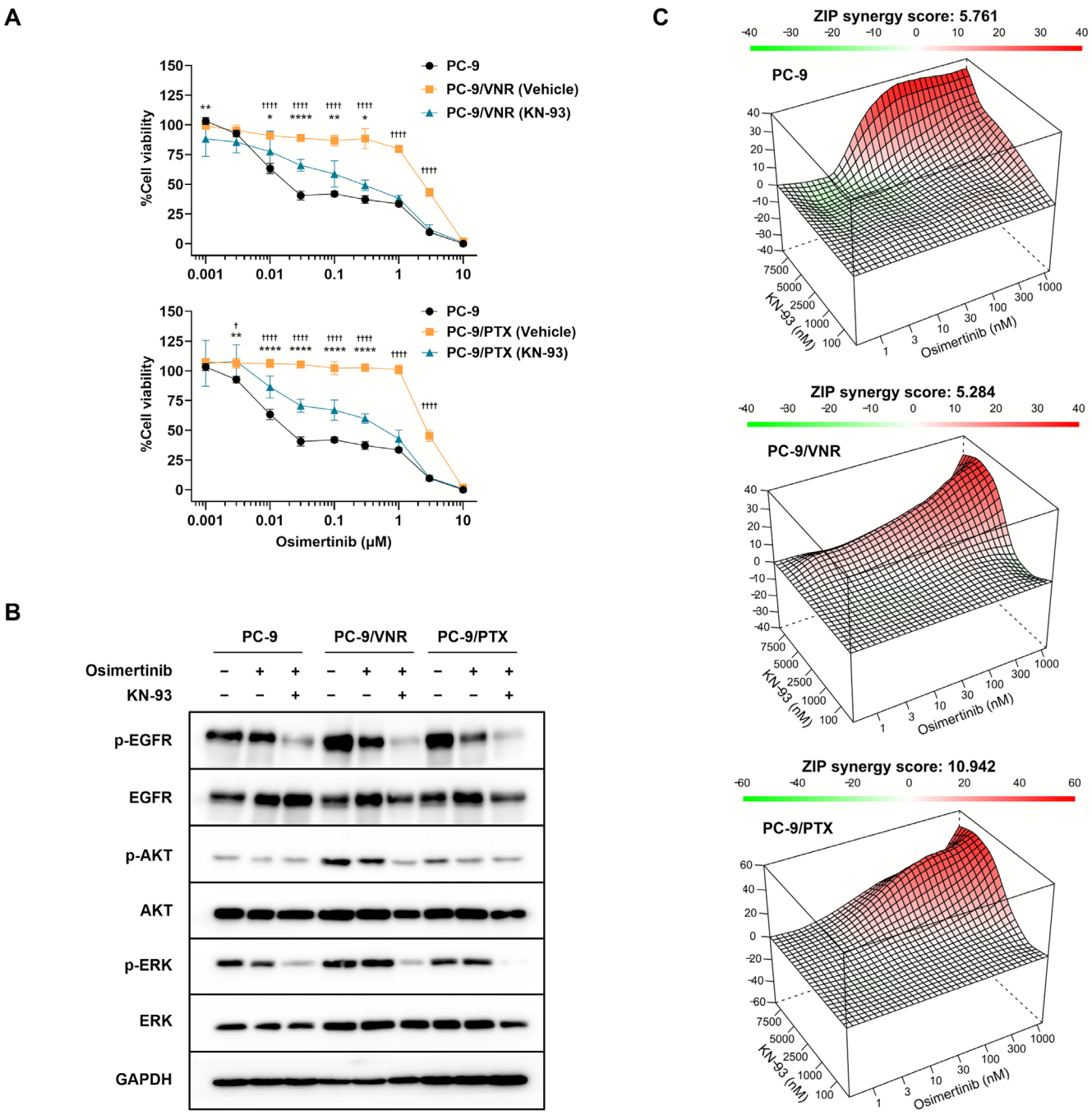

FIGURE 5 | Combination of osimertinib and KN-93 induces additive or synergistic effects in PC-9, PC-9/VNR, and PC-9/PTX cells. (A) Cell viability decreased in PC-9/VNR and PC-9/PTX cells under co-treatment with osimertinib and KN-93 (7.5 μM, 72 h), compared with osimertinib alone. (B) Co-treatment with KN-93 (7.5 μM, 24 h) and osimertinib (10 nM, 24 h) reduced phosphorylation of EGFR and downstream proteins in PC-9, PC-9/VNR, and PC-9/PTX cells. GAPDH was used as a loading control. (C) A synergistic effect of osimertinib and KN-93 was observed in PC-9/PTX cells, while additive effects were observed in PC-9 and PC-9/VNR cells. 3D synergy plots show drug interaction based on Zero Interaction Potency model calculations of 72-h viability data using SynergyFinder v3.0. Data are presented as mean ± SD ($n = 3$). Statistical significance: PC-9 versus PC-9/VNR (KN-93) or PC-9/PTX (KN-93), $^{*}p < 0.05$; $^{**}p < 0.01$; $^{***}p < 0.001$; $^{****}p < 0.0001$. PC-9 versus PC-9/VNR (Vehicle) or PC-9/PTX (Vehicle), $^{\dagger}p < 0.05$; $^{\dagger\dagger}p < 0.01$; $^{\dagger\dagger\dagger}p < 0.001$; $^{\dagger\dagger\dagger\dagger}p < 0.0001$.

CaMKII is known to regulate cancer cell proliferation and drug resistance by targeting multiple downstream effectors [29]. Notably, PC-9/VNR and PC-9/PTX cells displayed greater sensitivity to CaMKII inhibition, with additive and synergistic effects, respectively, compared to their parental PC-9 cells. Although the specific phenotypic alterations in PC-9/VNR and PC-9/PTX may differ from PC-9, our findings suggest a shift from reliance on EGFR autophosphorylation to FZD7/CaMKII signaling for proliferation under selective pressure from microtubule inhibitors. In contrast, no upregulation of the non-canonical Wnt signaling pathway was observed in H1975/VNR and H1975/PTX cells, suggesting that activation of this pathway

may depend on cellular and genetic backgrounds, including specific EGFR mutation subtypes. Further studies are warranted to examine alterations in non-canonical Wnt signaling across a broader range of NSCLC models.

In EGFR-mutated NSCLC, EGFR signaling serves as the primary oncogenic driver, making EGFR-TKIs a central therapeutic strategy [30]. However, resistance to EGFR-TKIs frequently arises through diverse mechanisms [31]. In this study, we demonstrated for the first time that the combination of KN-93 and osimertinib more effectively inhibited the proliferation of VNR- and PTX-treated NSCLC cells than either agent alone. Notably, the combination treatment also produced a greater reduction in EGFR phosphorylation than treatment with osimertinib monotherapy. Although the precise mechanism of inhibition remains unclear, our findings are consistent with previous reports suggesting that cytosolic Ca^{2+} can induce EGFR phosphorylation via direct binding to the EGFR protein [32], and that KN-93 combined with EGFR inhibitors (afatinib or cetuximab) attenuates EGFR signaling in oral squamous cell carcinoma [33]. Potential inducers of CaMKII-related ERK signaling, such as fibronectin or DUSPs, may contribute to ERK activation observed in PC-9/VNR and PC-9/PTX cells under EGFR inhibition by osimertinib [34, 35]. These results imply that CaMKII may play a role in the crosstalk between non-canonical Wnt and EGFR signaling pathways. While additional preclinical validation is needed, dual inhibition of CaMKII and EGFR may represent a novel therapeutic strategy to overcome cross-resistance in NSCLC cells previously exposed to tubulin inhibitors and EGFR-TKIs.

While adjuvant chemotherapy remains the standard of care for patients who have undergone complete resection of EGFR-mutated NSCLC, we explored alternative therapeutic strategies based on our findings of CaMKII-mediated cross-resistance to improve the survival outcomes. Our results suggest that the timing of EGFR-TKI administration within the treatment sequence should be reconsidered to optimize therapeutic efficacy. One potential strategy is to bypass standard post-surgical, microtubule-targeting adjuvant chemotherapy. However, such an approach must demonstrate benefits exceeding those of current adjuvant chemotherapy to warrant a shift in clinical practice [5]. Alternatively, administering EGFR-TKIs, traditionally reserved for treatment-naive EGFR-mutated tumors [19], as adjuvant therapy prior to microtubule inhibitors may help prevent the emergence of cross-resistance. Previous studies have shown that the therapeutic efficacy of chemotherapy does not differ significantly whether administered before or after EGFR-TKI treatment [36], which is a common treatment sequence among patients with advanced NSCLC. Furthermore, CaMKII-mediated multidrug resistance following EGFR-TKI treatment has not been reported. Another promising strategy is to individualize post-treatment regimens by identifying molecular subtypes of cross-resistance before initiating EGFR-TKI therapy, enabling more personalized interventions [37]. This approach will require further investigation into how adjuvant chemotherapy affects the efficacy of subsequent EGFR-TKI and other agents in patients with NSCLC. Moreover, preventing or overcoming cross-resistance remains a critical challenge [38, 39]. We investigated the combination of EGFR-TKIs and CaMKII inhibitors as a potential strategy to overcome acquired resistance to EGFR-TKIs. However, it is important to note that the clinical efficacy and adverse effects of CaMKII inhibitors remain unclear owing to their target selectivity. KN-93 has several targets in other kinases [40]. Moreover, osimertinib has been associated with QT prolongation [41], and systemic inhibition of CaMKII can affect cardiac ion channels and excitation–contraction coupling [42]. Therefore, concurrent inhibition of CaMKII and EGFR may increase the risk of cardiac toxicity. The development of CaMKII inhibitors with greater cancer-cell selectivity may thus be necessary for clinical applications. Considering the comparable efficacy observed in patients who did and did not receive prior adjuvant chemotherapy [6], omitting postoperative administration of microtubule inhibitors may be reasonable. Furthermore, administering microtubule inhibitors after EGFR-TKI treatment could potentially enhance therapeutic efficacy, provided their post-EGFR-TKI performance remained comparable to that observed with second-line use, which shows a response rate of approximately 30% [36].

This study has some limitations. Pemetrexed was only approved for postoperative chemotherapy in Japan in 2025 [43], preventing us from evaluating its efficacy during the study period. Although a combination of platinum and pemetrexed has demonstrated adjuvant efficacy equivalent to vinorelbine [37]; pemetrexed has also been reported to induce resistance to EGFR-TKIs [44, 45]. Therefore, further investigation is warranted to assess its impact on therapeutic sequencing. Additionally, this study was conducted entirely in vitro using cell line models, only in PC-9-derived cells with upregulation of the non-canonical Wnt/Ca^{2+} signaling pathway, which may not fully capture the complexity of tumor behavior and drug response in patients. The tumor microenvironment, immune interactions, and pharmacokinetics can significantly influence drug resistance mechanisms in vivo. Therefore, further validation using animal models and clinical samples is necessary to confirm the clinical relevance of our findings.

In summary, exposure of an EGFR-mutated NSCLC cell line to microtubule-targeting agents led to the upregulation of the FZD7/CaMKII signaling axis. Activation of CaMKII within this pathway appears to play a pivotal role in mediating acquired resistance to osimertinib. These findings highlight the importance of treatment sequence and suggest that the timing of EGFR-TKI administration should be carefully considered in the management of EGFR-mutated NSCLC.

Author Contributions

Kento Kono: data curation, formal analysis, investigation, visualization, writing – original draft. **Ryosuke Tanino:** data curation, formal analysis, investigation, methodology, project administration, validation, visualization, writing – review and editing. **Yukari Tsubata:** conceptualization, writing – review and editing. **Eshat Fahmida Haque:** writing – review and editing. **Takeshi Isobe:** project administration, supervision, writing – review and editing. **Tamio Okimoto:** project administration, supervision, writing – review and editing.

Acknowledgments

The authors have nothing to report.

Funding

This study was supported solely by internal departmental funds from the Division of Medical Oncology and Respiratory Medicine, Shimane University Faculty of Medicine. No external funding was received.

Ethics Statement

The authors have nothing to report.

Consent

The authors have nothing to report.

Conflicts of Interest

Yukari Tsubata has received honoraria from Chugai Pharmaceutical Co. Ltd., Daiichi Sankyo Co. Ltd., AstraZeneca PLC, Kyowa Kirin Co. Ltd., Taiho Pharmaceutical Co. Ltd., Bristol-Myers Squibb Co., and Takeda Pharmaceutical Co. Ltd. Takeshi Isobe has received honoraria from AstraZeneca PLC. All other authors declare no conflicts of interest.

References

1. J. Ferlay, M. Colombet, I. Soerjomataram, et al., "Cancer Statistics for the Year 2020: An Overview," *International Journal of Cancer* 149 (2021): 778–789, https://doi.org/10.1002/ijc.33588.

2. J. U. Lim and C. D. Yeo, "Update on Adjuvant Therapy in Completely Resected NSCLC Patients," *Thoracic Cancer* 13 (2022): 277–283, https://doi.org/10.1111/1759-7714.14277.

3. T. Miyoshi and M. Tsuboi, "Postoperative Adjuvant Therapy With Molecularly Targeted Agents for Non-Small Cell Lung Cancer," *International Journal of Clinical Oncology* 30 (2025): 210–214, https://doi.org/10.1007/s10147-024-02671-4.

4. J. Remon, C. E. Steuer, S. S. Ramalingam, and E. Felip, "Osimertinib and Other Third-Generation EGFR TKI in EGFR-Mutant NSCLC Patients," *Annals of Oncology* 29 (2018): i20–i27, https://doi.org/10.1093/annonc/mdx704.

5. M. Tsuboi, R. S. Herbst, T. John, et al., "Overall Survival With Osimertinib in Resected EGFR-Mutated NSCLC," *New England Journal of Medicine* 389 (2023): 137–147, https://doi.org/10.1056/NEJMoa2304594.

6. Y.-L. Wu, T. John, C. Grohe, et al., "Postoperative Chemotherapy Use and Outcomes From ADAURA: Osimertinib as Adjuvant Therapy for Resected EGFR-Mutated NSCLC," *Journal of Thoracic Oncology* 17 (2022): 423–433, https://doi.org/10.1016/j.jtho.2021.10.014.

7. D. Brazel and M. Nagasaka, "Deconstructing ADAURA. It Is Not Yet Time to Forgo Platinum-Based Adjuvant Chemotherapy in Resected Early Stage (IB-IIIA) EGFR-Mutant NSCLC," *Lung Cancer: Targets and Therapy* 13 (2022): 47–52, https://doi.org/10.2147/LCTT.S346922.

8. K. Onodera, I. Yokota, Y. Matsumura, et al., "Efficacy of Platinum-Based Adjuvant Chemotherapy for Epidermal Growth Factor Receptor-Mutant Lung Adenocarcinoma," *Journal of Thoracic Disease* 15 (2023): 6534–6543, https://doi.org/10.21037/jtd-23-1323.

9. M. B. D. Aldonza, J.-Y. Hong, M. V. Alinsug, J. Song, and S. K. Lee, "Multiplicity of Acquired Cross-Resistance in Paclitaxel-Resistant Cancer Cells Is Associated With Feedback Control of TUBB3 via FOXO3a-Mediated ABCB1 Regulation," *Oncotarget* 7 (2016): 34395–34419, https://doi.org/10.18632/oncotarget.9118.

10. T. Nakanishi, T. Menju, S. Nishikawa, et al., "The Synergistic Role of ATP-Dependent Drug Efflux Pump and Focal Adhesion Signaling Pathways in Vinorelbine Resistance in Lung Cancer," *Cancer Medicine* 7 (2018): 408–419, https://doi.org/10.1002/cam4.1282.

11. X. Wu, Q. Wu, X. Zhou, and J. Huang, "SphK1 Functions Downstream of IGF-1 to Modulate IGF-1-Induced EMT, Migration and Paclitaxel Resistance of A549 Cells: A Preliminary In Vitro Study," *Journal of Cancer* 10 (2019): 4264–4269, https://doi.org/10.7150/jca.32646.

12. C. Laface, F. M. Maselli, A. N. Santoro, et al., "The Resistance to EGFR-TKIs in Non-Small Cell Lung Cancer: From Molecular Mechanisms to Clinical Application of New Therapeutic Strategies," *Pharmaceutics* 15 (2023): 1604, https://doi.org/10.3390/pharmaceutics15061604.

13. A. Ianevski, A. K. Giri, and T. Aittokallio, "SynergyFinder 3.0: An Interactive Analysis and Consensus Interpretation of Multi-Drug Synergies Across Multiple Samples," *Nucleic Acids Research* 50 (2022): W739–W743, https://doi.org/10.1093/nar/gkac382.

14. M. L. P. Bueno, S. T. O. Saad, and F. M. Roversi, "WNT5A in Tumor Development and Progression: A Comprehensive Review," *Biomedicine & Pharmacotherapy* 155 (2022): 113599, https://doi.org/10.1016/j.biopha.2022.113599.

15. K. Qin, M. Yu, J. Fan, et al., "Canonical and Noncanonical Wnt Signaling: Multilayered Mediators, Signaling Mechanisms and Major Signaling Crosstalk," *Genes & Diseases* 11 (2024): 103–134, https://doi.org/10.1016/j.gendis.2023.01.030.

16. M. Sumi, K. Kiuchi, T. Ishikawa, et al., "The Newly Synthesized Selective Ca^{2+} Calmodulin Dependent Protein Kinase II Inhibitor KN-93 Reduces Dopamine Contents in PC12h Cells," *Biochemical and Biophysical Research Communications* 181 (1991): 968–975, https://doi.org/10.1016/0006-291X(91)92031-E.

17. C. N. Brown and K. U. Bayer, "Studying CaMKII: Tools and Standards," *Cell Reports* 43 (2024): 113982, https://doi.org/10.1016/j.celrep.2024.113982.

18. C. Zhou, Y.-L. Wu, G. Chen, et al., "Erlotinib Versus Chemotherapy as First-Line Treatment for Patients With Advanced EGFR Mutation-Positive Non-Small-Cell Lung Cancer (OPTIMAL, CTONG-0802): A Multicentre, Open-Label, Randomised, Phase 3 Study," *Lancet Oncology* 12 (2011): 735–742, https://doi.org/10.1016/S1470-2045(11)70184-X.

19. S. S. Ramalingam, J. Vansteenkiste, D. Planchard, et al., "Overall Survival With Osimertinib in Untreated, EGFR-Mutated Advanced NSCLC," *New England Journal of Medicine* 382 (2020): 41–50, https://doi.org/10.1056/NEJMoa1913662.

20. N. Vasan, J. Baselga, and D. M. Hyman, "A View on Drug Resistance in Cancer," *Nature* 575 (2019): 299–309, https://doi.org/10.1038/s41586-019-1730-1.

21. T. Winton, R. Livingston, D. Johnson, et al., "Vinorelbine Plus Cisplatin vs. Observation in Resected Non–Small-Cell Lung Cancer," *New England Journal of Medicine* 352 (2005): 2589–2597, https://doi.org/10.1056/NEJMoa043623.

22. J. He, J. Shen, C. Yang, et al., "Adjuvant Chemotherapy for the Completely Resected Stage IB Nonsmall Cell Lung Cancer: A Systematic Review and Meta-Analysis," *Medicine (Baltimore)* 94 (2015): e903, https://doi.org/10.1097/MD.0000000000000903.

23. T. Phesse, D. Flanagan, and E. Vincan, "Frizzled7: A Promising Achilles' Heel for Targeting the Wnt Receptor Complex to Treat Cancer," *Cancers* 8 (2016): 50, https://doi.org/10.3390/cancers8050050.

24. M. Casás-Selves, J. Kim, Z. Zhang, et al., "Tankyrase and the Canonical Wnt Pathway Protect Lung Cancer Cells From EGFR Inhibition," *Cancer Research* 72 (2012): 4154–4164, https://doi.org/10.1158/0008-5472.CAN-11-2848.

25. R. Yan, X. Fan, Z. Xiao, et al., "Inhibition of DCLK1 Sensitizes Resistant Lung Adenocarcinomas to EGFR-TKI Through Suppression of Wnt/β-Catenin Activity and Cancer Stemness," *Cancer Letters* 531 (2022): 83–97, https://doi.org/10.1016/j.canlet.2022.01.030.

26. B. Liang, Q. Wu, Y. Wang, et al., "Cdc42-Driven Endosomal Cholesterol Transport Promotes Collateral Resistance in HER2-Positive Gastric Cancer," *Cancer Letters* 587 (2024): 216702, https://doi.org/10.1016/j.canlet.2024.216702.

27. S. R. Sennoune, T. Nelius, C. Jarvis, K. Pruitt, K. R. Kottapalli, and S. Filleur, "The Wnt Non-Canonical Signaling Modulates Cabazitaxel Sensitivity in Prostate Cancer Cells," *PLoS One* 15 (2020): e0234078, https://doi.org/10.1371/journal.pone.0234078.

28. H. Zhang, X. Yang, F. Hu, et al., "Expression Level of Wnt5a Was Related to the Therapeutic Effects of First-Generation EGFR-TKIs," *Oncotargets and Therapy* 13 (2020): 5387–5394, https://doi.org/10.2147/OTT.S250024.

29. Q. He and Z. Li, "The Dysregulated Expression and Functional Effect of CaMK2 in Cancer," *Cancer Cell International* 21 (2021): 326, https://doi.org/10.1186/s12935-021-02030-7.

30. F. Zhou, H. Guo, Y. Xia, et al., "The Changing Treatment Landscape of EGFR-Mutant Non-Small-Cell Lung Cancer," *Nature Reviews. Clinical Oncology* 22 (2025): 95–116, https://doi.org/10.1038/s41571-024-00971-2.

31. J. Chmielecki, J. E. Gray, Y. Cheng, et al., "Candidate Mechanisms of Acquired Resistance to First-Line Osimertinib in EGFR-Mutated Advanced Non-Small Cell Lung Cancer," *Nature Communications* 14 (2023): 1070, https://doi.org/10.1038/s41467-023-35961-y.

32. P. Sánchez-González, K. Jellali, and A. Villalobo, "Calmodulin-Mediated Regulation of the Epidermal Growth Factor Receptor," *FEBS Journal* 277 (2010): 327–342, https://doi.org/10.1111/j.1742-4658.2009.07469.x.

33. Y. Lin, Y. Huang, B. Yang, et al., "Precision Therapy Targeting CAMK2 to Overcome Resistance to EGFR Inhibitors in FAT1-Mutated Oral Squamous Cell Carcinoma," *Chinese Medical Journal* 138 (2025): 1853–1865, https://doi.org/10.1097/CM9.0000000000003217.

34. M. Illario, A. L. Cavallo, K. U. Bayer, et al., "Calcium/Calmodulin-Dependent Protein Kinase II Binds to Raf-1 and Modulates Integrin-Stimulated ERK Activation," *Journal of Biological Chemistry* 278 (2003): 45101–45108, https://doi.org/10.1074/jbc.M305355200.

35. H.-F. Chen, H.-C. Chuang, and T.-H. Tan, "Regulation of Dual-Specificity Phosphatase (DUSP) Ubiquitination and Protein Stability," *International Journal of Molecular Sciences* 20 (2019): 2668, https://doi.org/10.3390/ijms20112668.

36. E. Miyauchi, A. Inoue, K. Kobayashi, et al., "Efficacy of Chemotherapy After First-Line Gefitinib Therapy in EGFR Mutation-Positive Advanced Non-Small Cell Lung Cancer – Data From a Randomized Phase III Study Comparing Gefitinib With Carboplatin Plus Paclitaxel (NEJ002)," *Japanese Journal of Clinical Oncology* 45 (2015): 670–676, https://doi.org/10.1093/jjco/hyv054.

37. M. Wang, R. S. Herbst, and C. Boshoff, "Toward Personalized Treatment Approaches for Non-Small-Cell Lung Cancer," *Nature Medicine* 27 (2021): 1345–1356, https://doi.org/10.1038/s41591-021-01450-2.

38. R. Loria, P. Vici, F. S. Di Lisa, S. Soddu, M. Maugeri-Saccà, and G. Bon, "Cross-Resistance Among Sequential Cancer Therapeutics: An Emerging Issue," *Frontiers in Oncology* 12 (2022): 877380, https://doi.org/10.3389/fonc.2022.877380.

39. C. Duan, M. Yu, J. Xu, B.-Y. Li, Y. Zhao, and R. K. Kankala, "Overcoming Cancer Multi-Drug Resistance (MDR): Reasons, Mechanisms, Nanotherapeutic Solutions, and Challenges," *Biomedicine & Pharmacotherapy* 162 (2023): 114643, https://doi.org/10.1016/j.biopha.2023.114643.

40. P. Pellicena and H. Schulman, "CaMKII Inhibitors: From Research Tools to Therapeutic Agents," *Frontiers in Pharmacology* 5 (2014): 21, https://doi.org/10.3389/fphar.2014.00021.

41. B. Khokhar, B. Chiang, K. Iglay, et al., "QT-Interval Prolongation, Torsades de Pointes, and Heart Failure With EGFR Tyrosine Kinase Inhibitors in Non-Small Cell Lung Cancer: Systematic Review," *Clinical Lung Cancer* 25 (2024): 285–318, https://doi.org/10.1016/j.cllc.2024.02.005.

42. T. J. Hund and P. J. Mohler, "Role of CaMKII in Cardiac Arrhythmias," *Trends in Cardiovascular Medicine* 25 (2015): 392–397, https://doi.org/10.1016/j.tcm.2014.12.001.

43. H. Kenmotsu, N. Yamamoto, T. Misumi, et al., "Five-Year Overall Survival Analysis of the JIPANG Study: Pemetrexed or Vinorelbine Plus Cisplatin for Resected Stage II-IIIA Nonsquamous Non–Small-Cell Lung Cancer," *Journal of Clinical Oncology* 41 (2023): 5242–5246, https://doi.org/10.1200/JCO.23.00179.

44. R. Tanino, Y. Tsubata, N. Harashima, M. Harada, and T. Isobe, "Novel Drug-Resistance Mechanisms of Pemetrexed-Treated Non-Small Cell Lung Cancer," *Oncotarget* 9 (2018): 16807–16821, https://doi.org/10.18632/oncotarget.24704.

45. X. Tong, R. Tanino, R. Sun, et al., "Protein Tyrosine Kinase 2: A Novel Therapeutic Target to Overcome Acquired EGFR-TKI Resistance in Non-Small Cell Lung Cancer," *Respiratory Research* 20 (2019): 270, https://doi.org/10.1186/s12931-019-1244-2.

Supporting Information

Additional supporting information can be found online in the Supporting Information section. **Figure S1:** H1975-derived cell lines treated with tubulin inhibitors (H1975/VNR and H1975/PTX) show no significant alterations in mRNA expression related to non-canonical Wnt signaling. **Table S1:** A list of differentially expressed genes in PC-9/VNR cells compared to the parental PC-9 cells. **Table S2:** A list of differentially expressed genes in PC-9/PTX cells compared to the parental PC-9 cells.